concentrations of L-Arg (5 to 100 mM) to muscles treated with L-NMMA and TNF-α resulted in a more pronounced negative inotropic effect than that seen with TNF-α alone [19 ± 4% of baseline tension with TNF-α and L-Arg as compared to 59 ± 7% of baseline tension with TNF-α alone ($P < 0.01$, $n = 6$; Student's two-tailed t test)] (Fig. 4A). This suggests that L-Arg enhanced the negative inotropic effect of TNF-α by providing additional substrate for NO production. This effect was also greater than that seen with L-Arg (100 mM) alone (31 ± 6% of baseline tension; $P < 0.01$, $n = 6$; Student's two-tailed t test). The addition of L-Arg (100 mM) to muscles treated with L-NMMA and IL-6 reduced tension to 35 ± 3% (Fig. 4B). The addition of L-Arg (100 mM) to muscles treated with L-NMMA and IL-2 reduced tension to 11 ± 10% of baseline (Fig. 4C). All of these inotropic effects were completely reversed within 30 min after the cytokines or other agents were washed away (Fig. 4, A through C). Removal of the endothelium did not alter the negative inotropic responses of the papillary muscles to cytokines (Fig. 4, A through C).

Cytokines increase the amount of NO in noncardiac tissues by inducing the transcription of an inducible NO synthase (*13–16*). The rapid onset and reversibility of the effects seen in this report argue against an effect requiring gene transcription. The negative inotropic effects of these cytokines in the papillary muscle preparation appear to result from enhanced activity of a constitutive NO synthase enzyme in the myocardium.

The observed inotropic effects of pro-inflammatory cytokines raise the possibility that they participate in reversible, postischemic myocardial depression ("stunning"). Myocardial stunning frequently occurs after cardiopulmonary bypass and may complicate successful recovery from cardiac surgery (*5–9*). We found elevated concentrations of IL-6 (1800 to 4000 U/ml) in bronchoalveolar fluid from patients after cardiopulmonary bypass (*18*). IL-6 also reversibly decreased tension generated by pectinate muscles removed from patients at the time of surgery (*18*). These preliminary observations in patients support the clinical relevance of our findings with the Syrian hamster papillary muscle preparation. Thus, the regulation of pro-inflammatory cytokines and myocardial NO synthase may provide new therapeutic strategies for the management of cardiac patients.

REFERENCES AND NOTES

1. J. Van Damme *et al.*, *J. Exp. Med.* **165**, 914 (1987).
2. R. D. Garman, K. A. Jacobs, S. C. Clark, D. H. Raulet, *Proc. Natl. Acad. Sci. U.S.A.* **84**, 7629 (1987).
3. A. Naldini, W. R. Fleischmann, Z. K. Ballas, K. D. Klimpel, G. R. Klimpel, *J. Immunol.* **139**, 1880 (1987).
4. B. Beutler and A. Cerami, *Annu. Rev. Immunol.* **7**, 625 (1989).
5. R. Engler and J. W. Covell, *Circ. Res.* **61**, 20 (1987).
6. B. R. Lucchesi, S. W. Werns, J. C. Fantone, *J. Mol. Cell. Cardiol.* **21**, 1241 (1989).
7. L. O. Go *et al.*, *Am. J. Physiol.* **255**, H1188 (1988).
8. W. Westlin and K. M. Mullane, *Circulation* **80**, 1828 (1989).
9. K. M. Mullane, W. Westlin, R. Kraemer, *Ann. N.Y. Acad. Sci.* **524**, 103 (1988).
10. R. M. J. Palmer, D. S. Ashton, S. Moncada, *Nature* **333**, 664 (1988).
11. L. J. Ignarro, G. M. Buga, K. S. Wood, R. E. Byrns, G. Chaudhuri, *Proc. Natl. Acad. Sci. U.S.A.* **84**, 9265 (1987).
12. S. Moncada *et al.*, *J. Cardiovasc. Pharmacol.* **17** (suppl. 3), S1 (1991).
13. S. J. Green, C. A. Nacy, M. S. Meltzer, *J. Leukocyte Biol.* **50**, 93 (1991).
14. D. J. Stuehr, H. J. Cho, N. S. Kwon, M. F. Weise, C. F. Nathan, *Proc. Natl. Acad. Sci. U.S.A.* **88**, 7773 (1991).
15. L. Li, R. G. Kilbourn, J. Adams, I. J. Fidler, *Cancer Res.* **51**, 2531 (1991).
16. S. S. Gross, E. A. Jaffe, R. Levi, R. G. Kilbourn, *Biochem. Biophys. Res. Commun.* **178** (no. 3), 823 (1991).
17. A. M. Shah, J. A. Smith, M. J. Lewis, *J. Cardiovasc. Pharmacol.* **17** (suppl. 3), S251 (1991).
18. B. G. Hattler and M. S. Finkel, paper presented at the 20th Annual Meeting of the Keystone Symposia on Molecular and Cellular Biology, Steamboat Springs, CO, 1 April 1991.
19. M. S. Finkel, L. Shen, R. C. Romeo, C. V. Oddis, G. Salama, *J. Cardiovasc. Pharmacol.* **19**, 610 (1992).
20. A. I. De'Agostini, S. C. Watkins, H. S. Slayter, H. Youssoufian, R. D. Rosenberg, *J. Cell Biol.* **111**, 1293 (1991).

21. Supported by awards from the American Heart Association, (Western) Pennsylvania Affiliate, the Sarah and David Weis Cardiovascular Research Fellowship, and NIH grant No. GM-37753. We thank B. A. Busch for assistance in the preparation of this manuscript.

16 March 1992; accepted 21 May 1992

Structure and Functional Expression of an ω-Conotoxin–Sensitive Human N-Type Calcium Channel

Mark E. Williams, Paul F. Brust, Daniel H. Feldman, Saraswathi Patthi, Susan Simerson, Azarnoush Maroufi, Ann F. McCue, Gönül Veliçelebi, Steven B. Ellis, Michael M. Harpold*

N-type calcium channels are ω-conotoxin (ω-CgTx)–sensitive, voltage-dependent ion channels involved in the control of neurotransmitter release from neurons. Multiple subtypes of voltage-dependent calcium channel complexes exist, and it is the α_1 subunit of the complex that forms the pore through which calcium enters the cell. The primary structures of human neuronal calcium channel α_{1B} subunits were deduced by the characterization of overlapping complementary DNAs. Two forms ($\alpha_{1B\text{-}1}$ and $\alpha_{1B\text{-}2}$) were identified in human neuroblastoma (IMR32) cells and in the central nervous system, but not in skeletal muscle or aorta tissues. The $\alpha_{1B\text{-}1}$ subunit directs the recombinant expression of N-type calcium channel activity when it is transiently co-expressed with human neuronal β_2 and α_{2b} subunits in mammalian HEK293 cells. The recombinant channel was irreversibly blocked by ω-CgTx but was insensitive to dihydropyridines. The $\alpha_{1B\text{-}1}\alpha_{2b}\beta_2$-transfected cells displayed a single class of saturable, high-affinity (dissociation constant = 55 pM) ω-CgTx binding sites. Co-expression of the β_2 subunit was necessary for N-type channel activity, whereas the α_{2b} subunit appeared to modulate the expression of the channel. The heterogeneity of α_{1B} subunits, along with the heterogeneity of α_2 and β subunits, is consistent with multiple, biophysically distinct N-type calcium channels.

Voltage-dependent Ca^{2+} channels are multisubunit complexes through which extracellular Ca^{2+} enters excitable cells. In rabbit skeletal muscle, four tightly coupled subunits, α_1, α_2, β, and γ, make up the channel complex (*1*). The primary structure of each subunit has been determined and α_1, α_2, and β cDNAs have been used to characterize transcripts expressed in other tissues (*2*). The α_1 and β subunits are each encoded by a gene family, including at least five distinct genes for α_1 subunits and three genes for β subunits (*3–6*). Primary transcripts of each of the α_1 genes, the α_2 gene, and two of the β genes have been shown to yield multiple, structurally distinct, subunits by means of differential processing (*6–9*). Expression studies have shown that the α_1 subunit forms the pore through which Ca^{2+} enters the cell (*10, 11*).

On the basis of biophysical and pharmacological characteristics, three subtypes of neuronal, high-voltage–activated Ca^{2+} channels (L-, N-, and P-type) have been proposed (*2*). These high-voltage–activated

SIBIA, Inc., 505 Coast Boulevard South, La Jolla, CA 92037.

*To whom correspondence should be addressed.

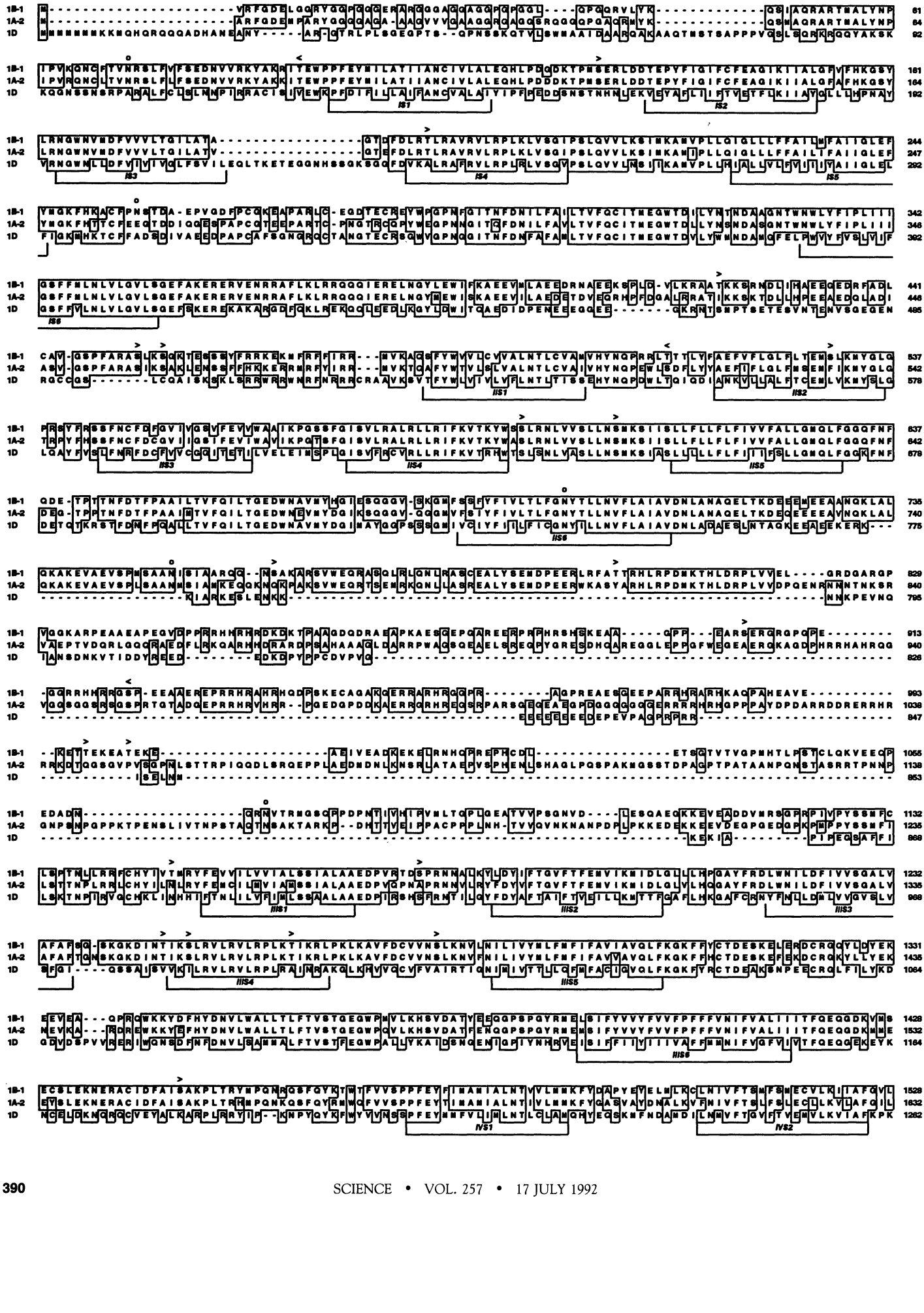
A
1B-1
1A-2
1D
IS1
IS2
IS3
IS4
IS5
IS6
IIS1
IIS2
IIS3
IIS4
IIS5
IIS6
IVS1
IVS2

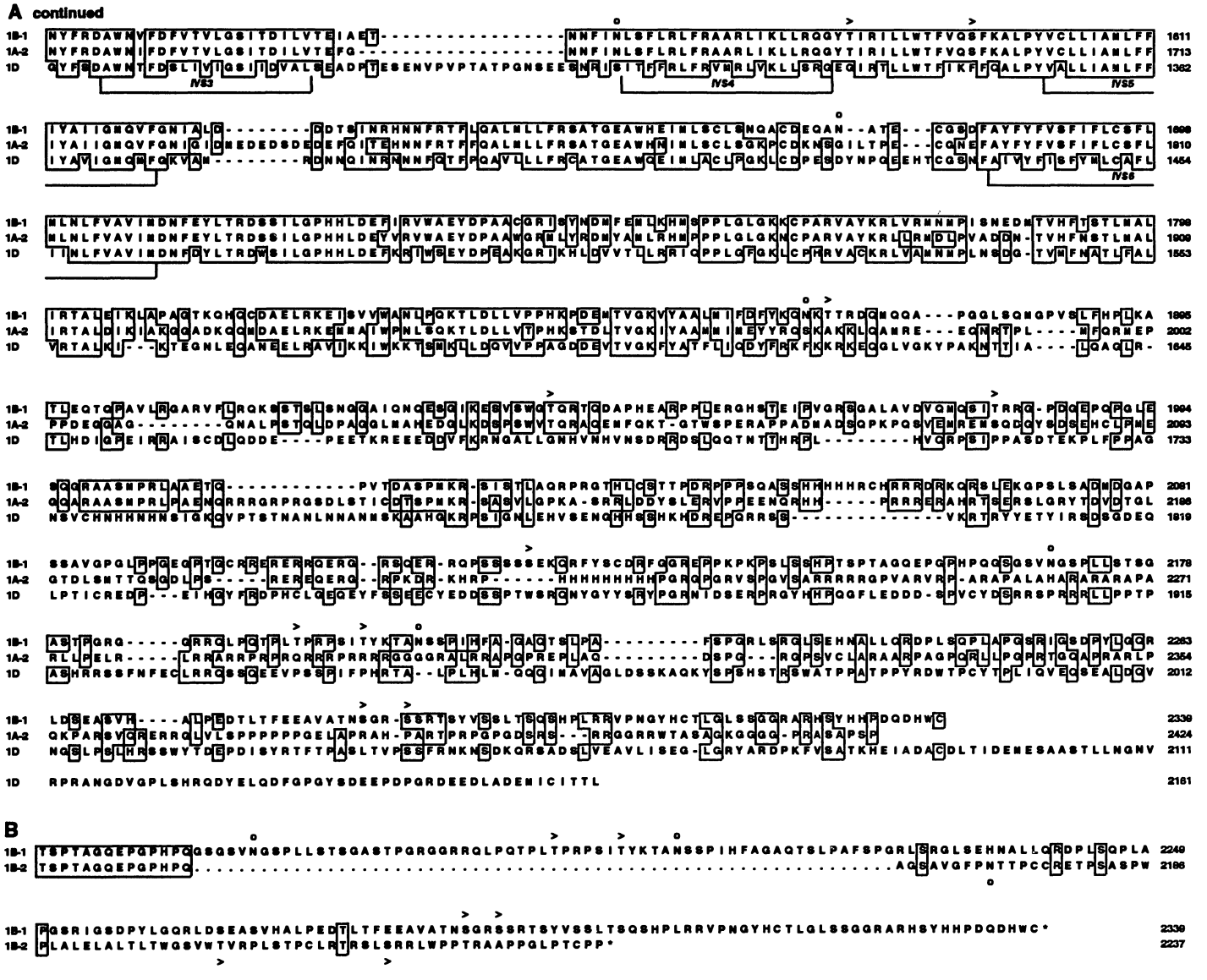

Fig. 1. Alignment of α_1 subunit deduced amino acid sequences. The nucleotide sequences have been deposited in GenBank (accession numbers M94172 and M94173 for $\alpha_{1B\text{-}1}$ and $\alpha_{1B\text{-}2}$, respectively). The number of the amino acid residue at the end of each line is given. Abbreviations for the amino acid residues are: A, Ala; C, Cys; D, Asp; E, Glu; F, Phe; G, Gly; H, His; I, Ile; K, Lys; L, Leu; M, Met; N, Asn; P, Pro; Q, Gln; R, Arg; S, Ser; T, Thr; V, Val; W, Trp; and Y, Tyr. Identical residues at one position in at least two of the sequences are enclosed in boxes. Potential *N*-glycosylation (○), cyclic adenosine monophosphate (AMP)–dependent phosphorylation (<), and protein kinase C phosphorylation (>) sites (*36*) are shown. (**A**) Alignment of functional, neuronal α_1 subunits; the amino acid sequences of the human neuronal Ca^{2+} channel $\alpha_{1B\text{-}1}$ (1B-1), the human neuronal α_{1D} (1D) (*8*), and the rabbit brain BI-2 (1A-2) (*11*) are shown. BI-2 is designated 1A-2 because it is a rabbit homolog of the rat brain class A gene (*4*). The numbering begins with the proposed initiating methionine. The putative transmembrane segments S1 through S6 in each of the repeats I through IV are shown (brackets). (**B**) Alignment of $\alpha_{1B\text{-}1}$ and $\alpha_{1B\text{-}2}$ sequences through the region of the insertion-deletion (*21*). The deduced amino acid sequence of the 187-nt insertion ($\alpha_{1B\text{-}1}$ nt 6490 to 6676; Gly^{2164} to Gly^{2226}) is shown.

subtypes are most readily distinguished pharmacologically. The neuronal L-type channel is dihydropyridine (DHP)-sensitive and, in some cases, reversibly blocked by ω-conotoxin (ω-CgTx) (*12, 13*), the N-type channel is DHP-insensitive and irreversibly blocked by ω-CgTx (*14*), and the P-type channel is both DHP- and ω-CgTx–insensitive but is sensitive to toxins in venom from funnel web spiders (*15*). Recently, recombinant expression of neuronal Ca^{2+} channels was used to identify a high-voltage–activated, DHP-sensitive Ca^{2+} channel that was reversibly blocked by ω-CgTx (classified as an L-type channel) (*8*) and a DHP-, ω-CgTx–insensitive Ca^{2+} channel (possibly a P-type channel) (*11*). Co-expression of α_1 and β subunits is necessary for substantial functional expression of both Ca^{2+} channel subtypes, whereas addition of an α_2 subunit increases the magnitude of the functional response.

Much evidence indicates that DHP-insensitive N-type Ca^{2+} channels that are irreversibly blocked by ω-CgTx are responsible for the voltage-activated release of neurotransmitters in many neurons (*16*). In addition, ω-CgTx binding sites have been localized to the frog neuromuscular presynaptic membrane (*17*) and to organized, single clusters coincident with synaptic contact sites in hippocampal neurons (*18*). Furthermore, ω-CgTx binding sites on the presynaptic membrane of the frog neuromuscular terminal align precisely with active zones where vesicular exocytosis of neurotransmitters occurs (*16, 17*). Finally, ω-CgTx irreversibly blocks Ca^{2+} currents recorded directly from presynaptic termi-

nals (*19*). We report here the complete amino acid sequence of a human neuronal α_1 subunit (designated α_{1B}) that mediates N-type voltage-dependent Ca^{2+} channel activity, which is irreversibly blocked by ω-CgTx when transiently co-expressed with the human neuronal α_{2b} and β_2 subunits (*8*) in human embryonic kidney (HEK) 293 cells. The transfected cells bind ω-CgTx with high affinity.

We previously reported the isolation of cDNAs that encode the α_1 subunit of the rabbit skeletal muscle DHP-sensitive, L-type Ca^{2+} channel (*3*). These cDNAs were used as probes to isolate overlapping cDNAs encoding a complete human neuronal α_{1B} subunit (*20*). The translation initiation site was assigned to the first in-frame methionine codon, and no upstream in-frame nonsense codon was identified (Fig. 1A). Two isoforms of α_{1B}, $\alpha_{1B\text{-}1}$ and $\alpha_{1B\text{-}2}$, that differ at their COOH-termini were identified (Fig. 1B). The $\alpha_{1B\text{-}1}$ subunit is comprised of 2339 amino acids and yields a calculated molecular weight of 262,494, whereas the $\alpha_{1B\text{-}2}$ subunit is comprised of 2237 amino acids and yields a calculated molecular weight of 251,757. These isoforms were identified by polymerase chain reaction (PCR) analysis (*21*) and revealed a deletion that produces $\alpha_{1B\text{-}2}$, which likely results from alternative selection of a splice acceptor. This insertion-deletion that produces different COOH-termini is similar to the processing of putative rabbit α_{1A} gene transcripts encoding the rabbit BI-1 and BI-2 isoforms that mediate DHP-, ω-CgTx–insensitive high-voltage–activated Ca^{2+} channel activity (*11*). The α_{1B} sequence is 94.5% identical to the previously reported 164–amino acid sequence deduced from a rat brain class B partial cDNA (*4*) and has the same transmembrane topology as described previously for other Ca^{2+} channel α_1 subunits (*7*).

The deduced amino acid sequences of two different neuronal α_1 subunits, the human α_{1D} (*8*) and the rabbit BI-2 (*11*), are shown aligned with the human $\alpha_{1B\text{-}1}$ sequence (Fig. 1A). The $\alpha_{1B\text{-}1}$ amino acid sequence is 64.1% and 43.0% identical to the BI-2 and α_{1D} sequences, respectively. The sequence identity is relatively well conserved through the four repeating domains, 72.6% and 50.7% for the $\alpha_{1B\text{-}1}$/BI-2 and the $\alpha_{1B\text{-}1}/\alpha_{1D}$ pairs, respectively. Both of the DHP-insensitive α_1 subunits, human neuronal $\alpha_{1B\text{-}1}$ and rabbit neuronal BI-2, have characteristic large putative cytoplasmic loops between the IIS6 and IIIS1 transmembrane domains. PCR analysis performed on RNAs isolated from IMR32 cells and several human primary tissues with $\alpha_{1B\text{-}1}$- and $\alpha_{1B\text{-}2}$-specific oligonucleotides identified $\alpha_{1B\text{-}1}$ and $\alpha_{1B\text{-}2}$ transcripts in IMR32 cells and in each of the human central nervous system (CNS) tissues tested, including hippocampus, habenula, and thalamus but not in human skeletal muscle or aorta tissues (*22*).

The transient expression of the human neuronal $\alpha_{1B\text{-}1}$, α_{2b}, and β_2 (*8*) subunits was studied in HEK293 cells (*23*). Transfected cells were examined for inward Ba^{2+} currents (I_{Ba}) mediated by voltage-dependent Ca^{2+} channels (*24*). Cells cotransfected with the $\alpha_{1B\text{-}1}$, α_{2b}, and β_2 cDNAs expressed high-voltage–activated Ca^{2+} channels (Fig. 2). I_{Ba} first appeared when the membrane was depolarized from a holding potential of −90 mV to −20 mV and peaked in magnitude at 10 mV. Thirty-nine of 95 cells (12 independent transfections) had I_{Ba} that ranged from 30 to 2700 pA, with a mean of 433 pA. The mean current density was 26 pA/pF, and the highest density was 150 pA/pF (*25*). The I_{Ba} typically increased by 2- to 20-fold during the first 5 min of recording. Repeated depolarizations during long recordings often revealed rundown of I_{Ba} usually not exceeding 20% within 10 min. I_{Ba} typically activated within 10 ms and inactivated with both a fast time constant ranging from 46 to 105 ms and a slow time constant ranging from 291 to 453 ms (n = 3). Inactivation showed a complex voltage dependence, such that I_{Ba} elicited at ≥20 mV inactivated more slowly than I_{Ba} elicited at lower test voltages, possibly a result of an increase in the magnitude of slow compared to fast inactivation components at higher test voltages.

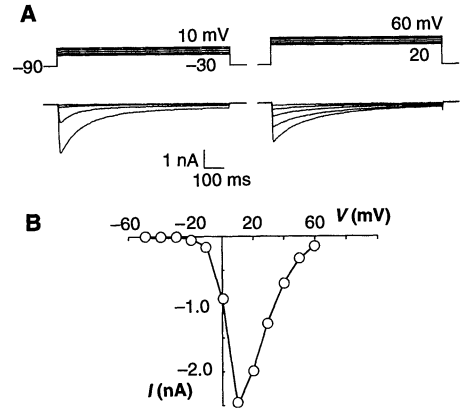

Fig. 2. Voltage dependence and kinetics of I_{Ba} expressed in HEK293 cells transfected with $\alpha_{1B\text{-}1}$, α_{2b}, and β_2 cDNAs (*23*). (**A**) Family of currents evoked at test voltages from −30 to 60 mV, from a holding potential of −90 mV. (**B**) Peak current-voltage relations measured from the currents in (A).

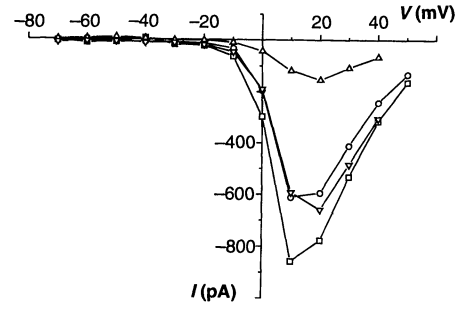

Fig. 3. Holding potential sensitivity of I_{Ba} expressed in HEK293 cells transfected with $\alpha_{1B\text{-}1}$, α_{2b}, and β_2 cDNAs (*23*). Peak current-voltage (*I-V*) relations measured from voltage steps delivered from different holding potentials (−90 mV, □; −70 mV, ○; −50 mV, △; return to −90 mV, ▽).

Recombinant $\alpha_{1B\text{-}1}\alpha_{2b}\beta_2$ channels were sensitive to holding potential (Fig. 3). Steady-state inactivation of I_{Ba}, measured after a 30- to 60-s conditioning at various holding potentials, was approximately 50% at holding potentials between −60 and −70 mV and approximately 90% at −40 mV. Recovery of I_{Ba} from inactivation was usually incomplete, measuring 55 to 75% of the original magnitude within 1 min after the holding potential was returned to more negative potentials, possibly indicating some rundown or a slow recovery rate.

Recombinant $\alpha_{1B\text{-}1}\alpha_{2b}\beta_2$ channels were also blocked irreversibly by ω-CgTx concentrations ranging from 0.5 to 10 μM during the time scale of the experiments (Fig. 4). Application of 5 μM toxin (n = 7) blocked the activity completely within 2 min, and we observed no recovery of I_{Ba} after washing ω-CgTx from the bath for up to 15 min. Cd^{2+} blockage (50 μM) was rapid, complete, and reversible; the DHPs Bay K 8644 (1 μM; n = 4) or nifedipine (5 μM; n = 3) had no discernable effect.

Cells cotransfected with cDNAs encoding $\alpha_{1B\text{-}1}$, α_{2b}, and β_2 subunits predominantly displayed a single class of saturable, high-affinity ω-CgTx binding sites (*26*) (Fig. 5). The determined dissociation constant (K_d) value (Fig. 5) was 54.6 ± 14.5 pM (n = 4). Cells transfected with the vector containing only β-galactosidase cDNA or $\alpha_{2b}\beta_2$ cDNA showed no specific binding. The binding capacity (B_{max}) of the $\alpha_{1B\text{-}1}\alpha_{2b}\beta_2$-transfected cells was 28,710 ± 11,950 sites per cell (n = 4).

These results demonstrate that $\alpha_{1B\text{-}1}$-$\alpha_{2b}\beta_2$-transfected cells express high-voltage–activated, inactivating Ca^{2+} channel activity that is irreversibly blocked by ω-CgTx, insensitive to DHPs, and sensitive to holding potential. The activation and inactivation kinetics and voltage sensitivity of the channel formed in these cells are generally consistent with previous characterizations of neuronal N-type Ca^{2+} channels (*27, 28*). Furthermore, the K_d value determined for ω-CgTx binding is in agreement with previously reported values (*29*).

The binding characteristics of ω-CgTx to HEK293 cells transiently expressing various subunit combinations were determined

from saturation binding analysis (Table 1). Each recombinant cell type displayed a single class of binding sites similar to the $\alpha_{1B\text{-}1}\alpha_{2b}\beta_2$-transfected cells, with K_d values ranging from 38.8 ± 13.1 pM to 76.1 ± 15.5 pM. The binding affinity of the recombinant cell types for ω-CgTx agrees well with that determined for intact IMR32 cells (36.5 ± 6.2 pM) (Table 1) but is different from measurements derived from crude homogenates of IMR32 cells (*30*).

There were significant differences in the receptor densities of the four recombinant cell types (Table 1). The B_{max} for ω-CgTx binding in $\alpha_{1B\text{-}1}\alpha_{2b}\beta_2$-type cells was approximately ten times greater than that in $\alpha_{1B\text{-}1}\alpha_{2b}$- and $\alpha_{1B\text{-}1}$-type cells. The estimate for the binding capacity of the IMR32 cells correlates well with a previous report (*30*). The comparison of the B_{max} values suggests that the ω-CgTx–binding $\alpha_{1B\text{-}1}$ subunit is more efficiently expressed on the cell surface when co-expressed with the α_{2b} and β_2 subunits. Similarly, efficient expression of heteromeric protein complexes on the cell surface, such as nicotinic acetylcholine receptors, has been shown to require subunit assembly (*31*).

We performed whole cell recordings of HEK293 cells transfected with the cDNA encoding $\alpha_{1B\text{-}1}$ or with cDNAs encoding $\alpha_{1B\text{-}1}$ and α_{2b} or β_2 to assess functional contributions of the various subunits to the N-type channel activity. Currents recorded from $\alpha_{1B\text{-}1}\beta_2$-transfected cells were observed at a frequency comparable to that of the $\alpha_{1B\text{-}1}\alpha_{2b}\beta_2$-transfected cells (16 of 46 cells; five independent transfections), consistent with a B_{max} of approximately 12,000 receptors per cell (Table 1). These currents resembled those observed in $\alpha_{1B\text{-}1}\alpha_{2b}\beta_2$-transfected cells, having similar current-voltage (*I-V*) curves, inactivation kinetics, and sensitivity to holding potential. Furthermore, $\alpha_{1B\text{-}1}\beta_2$-mediated currents were irreversibly blocked by ω-CgTx (5 μM; n = 3). However, currents in $\alpha_{1B\text{-}1}\beta_2$-transfected cells were generally smaller in magnitude than those observed in $\alpha_{1B\text{-}1}\alpha_{2b}\beta_2$ cells and never exceeded 205 pA (15 pA/pF), with a mean of 91 pA (5.6 pA/pF). In contrast, currents in $\alpha_{1B\text{-}1}\alpha_{2b}\beta_2$-transfected cells exceeded 200 pA in 57% of the cells tested (*25*).

Of 23 cells studied that were transfected with only $\alpha_{1B\text{-}1}$ (three independent transfections), two had small (20 to 40 pA) rapidly inactivating (τ = ~20 ms) currents that were reversibly blocked by ω-CgTx. A similar current was detected in 1 of 11 $\alpha_{1B\text{-}1}\alpha_{2b}$-transfected cells, whereas none of the untransfected HEK293 cells (n = 17) or HEK293 cells transiently expressing the α_{2b} and β_2 subunits (n = 17) displayed such currents. These results together with the relatively small B_{max} values observed in $\alpha_{1B\text{-}1}$-only and $\alpha_{1B\text{-}1}\alpha_{2b}$-transfected cells (<2650 receptors per cell) further support the importance of the β subunit in the formation of functional N-type Ca^{2+} channels.

N-type Ca^{2+} channels characterized from different cell preparations have biophysically distinct properties that have made it difficult to distinguish N- and L-type currents on the basis of inactivation properties. N-type Ca^{2+} channels were first described in chicken sensory neurons as high-voltage–activated Ca^{2+} channels that could be activated only from strongly negative holding potentials and inactivated within tens of milliseconds (*27*). Current remaining after decay of the inactivating component or currents activated from holding potentials ≥ −40 mV were believed to represent L-type channel activity. N-type Ca^{2+} channels have since been found to inactivate slowly and incompletely in some neuronal types (*32*). The range of inactivation rates observed in different tissues may be a result of a combination of factors, including distinct combinations of variant channel subunits and different states of regulation. Recent single channel analysis indicates that individual N-type channels can switch between transient and long-lasting modes of gating (*33*). Our whole cell data that show biphasic decay of a recombinantly expressed N-type Ca^{2+} channel are consistent with a population of channels that exhibit different gating modes.

Recent biochemical studies on brain ω-CgTx receptors have revealed proteins on SDS–polyacrylamide gel electrophoresis of a relative molecular mass consistent with α_1, α_2, and β subunits (*29*), although additional uncharacterized bands were also observed. Molecular biological evidence indicates that multiple α_1, α_2, and β transcripts, including α_{1B}, α_{2b}, and β_2 mRNAs, are co-expressed in IMR32 cells and hippocampal tissue (*8*), both sources of ω-CgTx binding sites (*18*, *30*). The recombinant expression of $\alpha_{1B\text{-}1}$, α_{2b}, and β_2 subunits to produce ω-CgTx–sensitive N-type channel activity confirms that an α_{1B} gene product mediates this activity. The functional necessity of a β subunit and modulation by an

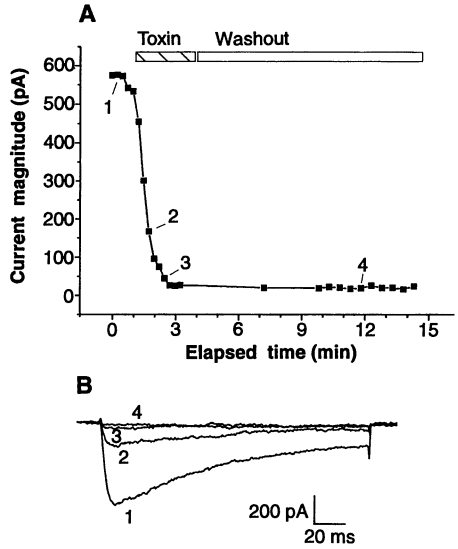

Fig. 4. Effect of ω-CgTx on I_{Ba} expressed in HEK293 cells transfected with $\alpha_{1B\text{-}1}$, α_{2b}, and β_2 cDNAs (*23*). (**A**) Plot of peak current magnitude versus time before, during (hatched bar), and after (open bar) application of 5 μM ω-CgTx. Test pulses (10 mV; holding potential = −90 mV) were delivered every 15 s before and during toxin application. Pulses were resumed every 30 s after recording of current-voltage relations from which only the current measured at 10 mV is shown. Similar results were obtained with the three concentrations of ω-CgTx tested: 0.5 μM (n = 3), 5 μM (n = 7), and 10 μM (n = 6). (**B**) Example recordings made at points 1 to 4 of (A).

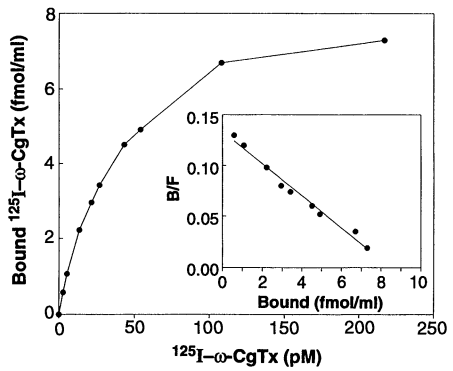

Fig. 5. Binding of ^{125}I–ω-CgTx. HEK293 cells were cotransfected with the $\alpha_{1B\text{-}1}$, α_{2b}, and β_2 cDNAs (*23*) and assayed for specific binding of ^{125}I–ω-CgTx as a function of increasing concentration of ^{125}I–ω-CgTx (*26*); 2 × 10^5 cells were used in the assay mixture. (Inset) Scatchard analysis of the data. B, bound; F, free.

Table 1. Summary of Scatchard analysis of ω-CgTx binding to intact cells. HEK293 cells transfected with the indicated subunit cDNAs and IMR32 cells induced with dibutyryl cyclic AMP and bromodeoxyuridine (*28*) were assayed for saturation of specific ω-CgTx binding, and the data were analyzed by the Scatchard method (*26*). The B_{max} values determined from Scatchard analysis were corrected for transfection efficiency.

Cell line	K_d (pM)	B_{max} (sites/cell)
$\alpha_{1B\text{-}1}\alpha_{2b}\beta_2$	54.6 ± 14.5	28,710 ± 11,950 (n = 4)
$\alpha_{1B\text{-}1}\beta_2$	38.8 ± 13.1	11,860 ± 5,910 (n = 4)
$\alpha_{1B\text{-}1}\alpha_{2b}$	76.1 ± 15.5	2,650 ± 620 (n = 4)
$\alpha_{1B\text{-}1}$	59.1 ± 15.5	2,085 ± 880 (n = 4)
IMR32	36.5 ± 6.2	6,770 ± 615 (n = 2)

α_2 subunit are consistent with the recombinant functional expression of other α_1 subtypes (*8*, *11*), although expression of $\alpha_{1B\text{-}1}$ alone appears sufficient for ω-CgTx binding.

Our results suggest that multiple subtypes of the N-type channel might exist as a result of the heterogeneity of the subunits that comprise the channel complex. Co-expression of three different β gene products with the rabbit cardiac (α_{1C}) subunit alters the channel properties and thus indicates that subunit composition can determine distinct, voltage-dependent Ca^{2+} channels (*6*). At least two forms each of α_{1B}, α_2, and β transcripts expressed in the brain are products of differential processing (*6*, *8*, *34*). This heterogeneity of the α_{1B}, α_2, and β subunits is consistent with biophysically distinct N-type channels characterized from different cell preparations. Recombinant expression of each of the α_{1B}, α_2, and β forms might reveal multiple N-type channels and the functional consequence of various subunit combinations (*35*).

REFERENCES AND NOTES

1. K. P. Campbell, A. T. Leung, A. H. Sharp, *Trends Neurosci.* **11**, 425 (1988).
2. R. J. Miller, *J. Biol. Chem.* **267**, 1403 (1992).
3. S. B. Ellis *et al.*, *Science* **241**, 1661 (1988).
4. T. P. Snutch, J. P. Leonard, M. M. Gilbert, H. A. Lester, N. Davidson, *Proc. Natl. Acad. Sci. U.S.A.* **87**, 3391 (1990); T. V. B. Starr, W. Prystay, T. P. Snutch, *ibid.* **88**, 5621 (1991).
5. E. Perez-Reyes *et al.*, *J. Biol. Chem.* **267**, 1792 (1992).
6. R. Hullin *et al.*, *EMBO J.* **11**, 885 (1992).
7. R. W. Tsien, P. T. Ellinor, W. A. Horne, *Trends Pharmacol. Sci.* **12**, 349 (1991).
8. M. E. Williams *et al.*, *Neuron* **8**, 71 (1992).
9. M. Pragnell, J. Sakamoto, S. D. Jay, K. P. Campbell, *FEBS Lett.* **291**, 253 (1991).
10. A. Mikami *et al.*, *Nature* **340**, 230 (1989).
11. Y. Mori *et al.*, *ibid.* **350**, 398 (1991).
12. T. Aosaki and H. Kasai, *Pfluegers Arch.* **414**, 150 (1989).
13. D. Swandulla, E. Carbone, H. D. Lux, *Trends Neurosci.* **14**, 46 (1991).
14. E. Sher and F. Clementi, *Neuroscience* **42**, 301 (1991).
15. R. Llinàs, M. Sugimori, J. W. Lin, B. Cherksey, *Proc. Natl. Acad. Sci. U.S.A.* **86**, 1689 (1989); I. M. Mintz *et al.*, *Nature* **355**, 827 (1992).
16. S. J. Smith and G. J. Augustine, *Trends Neurosci.* **11**, 458 (1988).
17. R. Robitaille, E. M. Adler, M. P. Charlton, *Neuron* **5**, 773 (1990); M. W. Cohen, O. T. Jones, K. J. Angelides, *J. Neurosci.* **11**, 1032 (1991); F. T. Tarelli, M. Passafaro, F. Clementi, E. Sher, *Brain Res.* **547**, 331 (1991).
18. O. T. Jones, D. L. Kunze, K. J. Angelides, *Science* **244**, 1189 (1989).
19. E. F. Stanley and G. Goping, *J. Neurosci.* **11**, 985 (1991).
20. Recombinant cDNA libraries were prepared, and overlapping $\alpha_{1B\text{-}1}$ cDNA clones were isolated from IMR32, human hippocampus, and basal ganglia cDNA libraries and characterized essentially as described (*3*, *8*).
21. We performed PCR analyses as described (*8*) using IMR32 RNA, human hippocampus RNA, and human genomic DNA with $\alpha_{1B\text{-}1}$-specific primers [nucleotides (nt) 6368 to 6391 and the complement of nt 7071 to 7095] to confirm the α_{1B} termination codon. The RNAs gave the expected 728-bp fragment ($\alpha_{1B\text{-}1}$) as well as a 541-bp fragment ($\alpha_{1B\text{-}2}$). The genomic DNA product was ~1350 bp. The DNA sequences of $\alpha_{1B\text{-}1}$ and $\alpha_{1B\text{-}2}$ diverge from each other after nt 6489. The $\alpha_{1B\text{-}1}$ subunit contains an additional 187-bp exon that alters the reading frame. After this exon, the $\alpha_{1B\text{-}1}$ and $\alpha_{1B\text{-}2}$ sequences are identical for the remaining 419 nucleotides characterized from both sequences, $\alpha_{1B\text{-}1}$ nt 6677 to 7095 and $\alpha_{1B\text{-}2}$ nt 6490 to 6908. The presence of the exon ($\alpha_{1B\text{-}1}$) results in the termination of the coding sequence at nt 7018 to 7020 (TAG); the absence of the exon ($\alpha_{1B\text{-}2}$) results in the termination of the coding sequence at nt 6712 to 6714 (TGA). Differential processing of the α_{1B} primary transcript was confirmed by characterization of the α_{1B} genomic PCR product. An ~270-bp intron was identified between $\alpha_{1B\text{-}1}$ nt 6489 and 6490. The $\alpha_{1B\text{-}1}$ and $\alpha_{1B\text{-}2}$ transcripts result from alternative selection of splice acceptor sites. $\alpha_{1B\text{-}1}$ is formed by selection of the splice acceptor at the intron-exon boundary, at nt 6490 on the exon side of the boundary; $\alpha_{1B\text{-}2}$ is formed by selection of a splice acceptor identified by an AG dinucleotide at nt 6675 and 6676 of the $\alpha_{1B\text{-}1}$ coding sequence.
22. Tissue distribution of the $\alpha_{1B\text{-}1}$ and $\alpha_{1B\text{-}2}$ transcripts was determined by PCR assays with oligonucleotide primers, nt 6447 to 6470 (Pro^{2149} to Glu^{2157}), and the complement of $\alpha_{1B\text{-}1}$-specific nt 6819 to 6843 (Leu^{2273} to Glu^{2281}). PCR products were probed with an $\alpha_{1B\text{-}1}$-specific oligonucleotide (nt 6513 to 6536; Ser^{2171} to Ala^{2179}) and an $\alpha_{1B\text{-}2}$-specific oligonucleotide (nt 6480 to 6498; Pro^{2160} to Ser^{2166}). The expected size bands were 396 bp ($\alpha_{1B\text{-}1}$) and 209 bp ($\alpha_{1B\text{-}2}$).
23. pcDNA$\alpha_{1B\text{-}1}$ was constructed in pcDNA1 (Invitrogen, San Diego, CA) with α1.179 (nt −143 to 2194), α1.177 (nt 2194 to 4160), α1.201 (nt 4160 to 5305), α1.200 (nt 5305 to 6116), and α1.230 (nt 6116 to 7176). DNA sequence analysis revealed that α1.177 has a two-nucleotide deletion (nt 3711 to 3712; Ser^{1237}) that was corrected with a PCR-amplified IMR32 Nar I–Kpn I fragment (nt 3685 to 4160; Gly^{1229} to Gly^{1387}). pHBCaCHα_{2b}(A) and pHBCaCHβ_{2b}.RBS(A), full-length α_{2b} and β_2 constructs in pcDNA1, were described previously (*8*). HEK293 cells [B. W. Stillman and Y. Gluzman, *Mol. Cell. Biol.* **5**, 2051 (1985)] were grown as a monolayer culture in Dulbecco's modified Eagle's medium (Gibco) containing 5% defined-supplemented bovine calf serum (Hyclone) plus penicillin G (100 U/ml) and streptomycin sulfate (100 μg/ml). HEK293 cell transfections were mediated by calcium phosphate [F. M. Ausubel *et al.*, Eds., *Current Protocols in Molecular Biology* (Wiley, New York, 1990), pp. 9.1.1 to 9.1.7]. Cells were transfected (2×10^6 per polylysine-coated plate). Standard transfections (10-cm dish) contained 8 μg of pcDNA$\alpha_{1B\text{-}1}$, 5 μg of pHBCaCHα_{2b}(A), 2 μg of pHBCaCHβ_{2b}.RBS(A), 2 μg of pCMVβ (Clontech β-galactosidase expression plasmid), and pUC18 to maintain a constant mass of 20 μg/ml. Cells were analyzed 48 to 72 hours after transfection. Transfection efficiencies (±10%) were determined by in situ histochemical staining for β-galactosidase activity [J. R. Sanes, J. L. R. Rubenstein, J.-F. Nicolas, *EMBO J.* **5**, 3133 (1986)]. Transfection efficiencies generally were >50%.
24. Properties of recombinantly expressed Ca^{2+} channels were studied by whole cell patch-clamp techniques [O. P. Hamill, A. Marty, E. Neher, B. Sakmann, F. J. Sigworth, *Pfluegers Arch.* **391**, 85 (1981)]. Recordings were performed on transfected HEK293 cells 2 to 3 days after transfection. Cells were plated at 100,000 to 300,000 cells per polylysine-coated, 35-mm tissue culture dishes (Falcon, Oxnard, CA) 24 hours before recordings. Cells were perfused with 15 mM $BaCl_2$, 125 mM choline chloride, 1 mM $MgCl_2$, and 10 mM Hepes (pH = 7.3) adjusted with tetraethylammonium hydroxide (bath solution). Pipettes were filled with 135 mM CsCl, 10 mM EGTA, 10 mM Hepes, 4 mM Mg–adenosine triphosphate (pH = 7.5) adjusted with tetraethylammonium hydroxide. Sylgard (Dow-Corning, Midland, MI)-coated, fire-polished, and filled pipettes had resistances of 1 to 2 megohm before we established gigohm seals to cells. ω-CgTx (Bachem), Bay K 8644, and nifedipine (Research Biochemicals, Natick, MA) were prepared as described (*8*), dissolved in bath solution, and continuously applied by means of puffer pipettes as required for a given experiment. Recordings were performed at room temperature (22° to 25°C). Series resistance compensation (70 to 85%) was employed to minimize voltage error that resulted from pipette access resistance, typically 2 to 3.5 megohm. Current signals were filtered (−3 dB, 4-pole Bessel) at a frequency of 1/4 to 1/5 the sampling rate, which ranged from 0.5 to 3 kHz. Voltage commands were generated, and data were acquired with CLAMPEX (pClamp, Axon Instruments, Foster City, CA). All data shown are corrected for linear leak and capacitive components as described (*8*). Exponential fitting of currents was performed with CLAMPFIT (Axon).
25. Currents <30 pA were not included because of unreliable measurements. For $\alpha_{1B\text{-}1}\alpha_{2b}\beta_2$-transfected cells, currents in 43.6% of the expressing cells ranged from 30 to 200 pA, 43.6% of the cells had currents that ranged from 200 to 1000 pA, and 12.8% had currents that exceeded 1000 pA.
26. We mechanically removed cells from tissue culture plates 48 hours after transfection by spraying with phosphate-buffered saline that contained 0.1% (w/v) bovine serum albumin (BSA). The cells were collected, washed once, and resuspended in assay buffer [10 mM Hepes (pH 7.4), 140 mM NaCl, 5 mM KCl, 12 mM glucose, and BSA (1 mg/ml)]. Specific binding of ^{125}I–ω-CgTx to transfected cells was determined as described (*30*) with several modifications. Briefly, we performed the assay in 12 mm × 75 mm polypropylene tubes in 0.5 ml of assay buffer by incubating the cells with 100 pM ^{125}I–ω-CgTx (DuPont Biotechnology Systems; 2200 Ci/mmol) for 1 hour at 37°C. Subsequently, 2 ml of ice-cold wash buffer [5 mM Hepes (pH 7.4), 160 mM choline chloride, 1.5 mM $CaCl_2$, and BSA (1 mg/ml)] was added to each tube, and the mixtures were centrifuged at 2300*g* for 30 min at 4°C. The pellets were washed again and counted for radioactivity. Nonspecific binding was determined in the presence of 20 nM unlabeled ω-CgTx. The optimum cell number was determined by a titration of 1×10^5 to 2×10^6 cells per assay tube. For saturation binding studies, the binding of ^{125}I–ω-CgTx was measured as a function of increasing concentration of ^{125}I–ω-CgTx. Nonspecific binding was subtracted at each concentration. Specific binding was plotted as a function of ^{125}I–ω-CgTx concentration and analyzed by the Scatchard method.
27. M. C. Nowycky, A. P. Fox, R. W. Tsien, *Nature* **316**, 440 (1985); A. P. Fox, M. C. Nowycky, R. W. Tsien, *J. Physiol.* (*London*) **394**, 149 (1987).
28. E. Carbone, E. Sher, F. Clementi, *Pfluegers Arch.* **416**, 170 (1990).
29. J. A. Wagner, A. M. Snowman, A. Biswas, B. M. Olivera, S. H. Snyder, *J. Neurosci.* **8**, 3354 (1988); J. Sakamoto and K. P. Campbell, *J. Biol. Chem.* **266**, 18914 (1991); M. K. Ahlijanian, J. Striessnig, W. A. Catterall, *ibid.*, p. 20192; M. W. McEnery, A. M. Snowman, A. H. Sharp, M. E. Adams, S. H. Snyder, *Proc. Natl. Acad. Sci. U.S.A.* **88**, 11095 (1991).
30. E. Sher, A. Pandiella, F. Clementi, *FEBS Lett.* **235**, 178 (1988).
31. P. Blount, M. M. Smith, J. P. Merlie, *J. Cell Biol.* **111**, 2601 (1990).
32. M. R. Plummer, D. E. Logothetis, P. Hess, *Neuron* **2**, 1453 (1989); S. W. Jones and T. N. Marks, *J. Gen. Physiol.* **94**, 169 (1989).
33. M. R. Plummer and P. Hess, *Nature* **351**, 657 (1991).
34. H.-L. Kim, H. Kim, P. Lee, R. G. King, H. Chin, *Proc. Natl. Acad. Sci. U.S.A.* **89**, 3251 (1992).
35. The amino acid sequence of a rat α_1 subunit, rbB-I, has been reported [S. J. Dubel *et al.*, *Proc. Natl. Acad. Sci. U.S.A.* **89**, 5058 (1992)] and is 92.8% identical to that of the human $\alpha_{1B\text{-}1}$ subunit. However, attempts to express the cDNA encoding the rbB-I protein did not yield functional Ca^{2+} channels, thus supporting our conclusion that additional subunits, such as β_2 and α_{2b}, are

required for functional expression.
36. E. Bause, *Biochem. J.* **209**, 331 (1983); D. B. Glass, M. R. El-Maghrabi, S. J. Pilkis, *J. Biol. Chem.* **261**, 2987 (1986); J. R. Woodgett, K. L. Gould, T. Hunter, *Eur. J. Biochem.* **161**, 177 (1986).
37. We thank K. Payne for thoughtful secretarial assistance, G. Holtz for computer assistance, and S. Wagner for providing CNS polyadenylated RNAs. We also thank V. Dionne, R. Evans, S. Heinemann, C. Liaw, R. Miller, P. Schoeneck, and S. Wagner for helpful discussions regarding this work.

15 May 1992; accepted 11 June 1992

Membrane Depolarization Induces p140^{trk} and NGF Responsiveness, But Not p75^{LNGFR}, in MAH Cells

Susan J. Birren, Joseph M. Verdi, David J. Anderson*

Nerve growth factor (NGF) is required for the maturation and survival of sympathetic neurons, but the mechanisms controlling expression of the NGF receptor in developing neuroblasts have not been defined. MAH cells, an immortalized sympathoadrenal progenitor cell line, did not respond to NGF and expressed neither low-affinity NGF receptor (p75) nor p140^{trk} messenger RNAs. Depolarizing concentrations of potassium chloride, but none of a variety of growth factors, induced expression of p140^{trk} but not p75 messenger RNA. A functional response to NGF was acquired by MAH cells under these conditions, suggesting that expression of p75 is not essential for this response. Depolarization also permitted a relatively high proportion of MAH cells to develop and survive as neurons in fibroblast growth factor and NGF. These data establish a relation between electrical activity and neurotrophic factor responsiveness in developing neurons, which may operate in the functioning of the mature nervous system as well.

The survival of vertebrate neurons is dependent on neurotrophic factors secreted by their postsynaptic targets. NGF, the prototypic neurotrophic factor, is required for the survival of sympathetic and some sensory neurons (*1*). The embryonic precursors to sympathetic neurons neither respond to nor require NGF (*2–4*). This raises the question of how developing sympathetic neuroblasts acquire their responsiveness to and dependence on NGF. We have studied this process with the use of MAH cells a retrovirally immortalized sympathoadrenal progenitor cell line (*5*). The identification of the product of the proto-oncogene *trk*, p140^{trk} (Trk), as a signal-transducing subunit of the NGF receptor (NGFR) (*6, 7*) has allowed us to use Trk mRNA expression to assay environmental signals that may induce NGF responsiveness in MAH cells. Here we identify membrane depolarization as one such signal.

MAH cells, like the nonimmortalized progenitors from which they derive, do not undergo neuronal differentiation in response to NGF. The protein p75, the low-affinity NGFR (*8, 9*), is not expressed by these cells (*5*). MAH cells grown in the absence of added factors also express little or no Trk mRNA (Fig. 1A, lanes 1 and 2). Thus, the failure of these precursor cells to respond to NGF correlates with their lack of expression of both types of NGFR mRNAs. We then sought to identify factors that induce expression of NGFR and NGF responsiveness. Previously, we found that basic fibroblast growth factor (bFGF) induced low levels of p75 expression and NGF responsiveness in a small subpopulation of MAH cells (*5*). However, bFGF failed to induce significant Trk expression in MAH cells, as did a number of other growth and neurotrophic factors (Fig. 1A, lanes 4 through 7, and data not shown). In addition, retinoic acid, which induces high-affinity NGF receptors and NGF dependence in chick sympathetic neuroblasts (*10*), did not induce Trk mRNA (Fig. 1A, lane 8).

In the chick, depolarization increases the survival of NGF-dependent sympathetic neurons (*4*). In MAH cells, depolarization stimulated the survival of postmitotic neurons. Depolarization of MAH cells produced by the addition of 40 mM KCl led to an induction of Trk mRNA (Fig. 1A, lane 3). A time course in 40 mM KCl revealed that Trk expression was detectable within 24 hours and reached maximal amounts within 3 days (Fig. 1C, lanes 5 through 8). Reprobing of the same blots with p75 probes revealed that, in contrast to Trk mRNA, p75 mRNA was not induced by 40 mM KCl.

MAH cells require dexamethasone (dex) for long-term survival; when dex is removed, the cells die within 4 to 5 days. In the presence of 5 μM dex, a low steady-state amount of Trk mRNA was detected (Fig. 1B, lane 2). However, even in the presence of dex an up-regulation of Trk mRNA by 40 mM KCl occurred (Fig. 1B, lane 3), indicating that the effect of depolarization is not simply to maintain the survival of Trk-expressing MAH cells. The time course of Trk induction by 40 mM KCl was similar in the presence of dex (Fig. 1D, lanes 6 through 9) as in its absence, although higher steady-state amounts of Trk mRNA were produced in the presence of dex (compare Fig. 1D, lane 8, with Fig. 1C, lane 7). As was the case in the absence of dex, no induction of p75 mRNA was detected in 40 mM KCl plus dex.

The effect of 40 mM KCl is likely to be produced by membrane depolarization because no induction of Trk mRNA was observed in 40 mM NaCl (Fig. 1, A and B, lanes 9). Moreover, veratridine, an Na^+ channel agonist that leads to membrane depolarization, also caused an increase in the amount of Trk mRNA concentrations (data not shown). In PC12 cells, the induction of immediate-early gene expression by membrane depolarization requires the opening of voltage-gated Ca^{2+} channels and depends on extracellular Ca^{2+} (*11*). Removal of extracellular Ca^{2+} or addition of dihydropyridine antagonists of voltage-gated Ca^{2+} channels resulted in the death of MAH cells within 24 hours, precluding our ability to determine a requirement for Ca^{2+} influx in Trk induction. However, at suboptimal concentrations of KCl (20 mM) (Fig. 1E, lane 4), the Ca^{2+} channel agonist Bay K 8644 potentiated the induction of Trk mRNA (Fig. 1F, lanes 3 and 4), which suggests that Ca^{2+} influx through voltage-gated L-type Ca^{2+} channels is indeed involved in the induction of Trk mRNA by membrane depolarization.

We then sought to determine whether depolarization induces a functional response to NGF. We used two assays of NGF responsiveness: neurite outgrowth and cell number. Cell number reflects both the survival- and proliferation-promoting (*12*) effects of NGF, although for technical reasons it is difficult to determine the relative contributions of these two processes in this system. NGF responses were assayed after 5 days, by which time most MAH cells had died in control medium (Table 1). Those few cells that survived showed little process outgrowth (Fig. 2A). Similar results were obtained in NGF alone (Fig. 2B and Table 1), indicating that MAH cells do not respond to this factor. Cell number was significantly increased by depolarizing concentrations of KCl (Table 1), although little neurite outgrowth was observed (Fig. 2C). In NGF plus 40 mM KCl, cell number was even higher (Table 1) and the cells bore long neurites (Fig. 2D). These neurite-bearing cells, however, lacked the cell soma hypertrophy characteristic of mature neu-

S. J. Birren, Division of Biology, California Institute of Technology, Pasadena, CA 91125.
J. M. Verdi and D. J. Anderson, Division of Biology and the Howard Hughes Medical Institute, California Institute of Technology, Pasadena, CA 91125.
*To whom correspondence should be addressed.